International Journal of Thermal Sciences 84 (2014) 9–20

Contents lists available at ScienceDirect

International Journal of Thermal Sciences

journal homepage: www.elsevier.com/locate/ijts

Numerical studies on damping of thermal waves

Min-Kai Zhang, Bing-Yang Cao*, Yin-Cheng Guo

Department of Engineering Mechanics, Tsinghua University, Beijing 100084, China

ARTICLE INFO

Article history:
Received 17 September 2013
Received in revised form
10 April 2014
Accepted 19 April 2014
Available online 2 June 2014

Keywords:
Thermal wave
Damping
Cattaneo–Vernotte model
Dual-phase-lagging model
Thermomass model

ABSTRACT

The damping levels of the temperature and heat flux (ε_T, ε_q) and the damping factor (ξ) were defined for evaluating and determining the damping of the thermal waves predicted by the Cattaneo–Vernotte (CV), dual-phase-lagging (DPL), and thermomass (TM) models. Numerical analyses were performed in terms of the three models. The damping level of the heat flux, instead of the temperature, is found to be a better evaluation factor because the heat flux is directly related to the energy transported by the thermal wave while the temperature can be also affected by the thermal properties. The damping factor ξ ($L/\sqrt{\alpha\tau}$) represents the ratio of the time that the thermal wave needs to travel the distance L to the relaxation time, or $\sqrt{3}$ times of the reciprocal of the Knudsen number, where L is the travelling distance of the thermal wave, α is the thermal diffusivity, and τ is the relaxation time. For the sharp thermal waves predicted by the CV and simplified TM models, the damping factors ξ_{CV} and ξ_{TM} can be the characteristic numbers that has a decisive impact on the damping level of the heat flux. But if both including the sharp and blunt thermal waves, the increase of overdamped cases under the blunt thermal wave situation will lead to the deviation for the characteristic numbers. For the sharp thermal waves predicted by the DPL and TM models, the damping factors ξ_{DPL} and ξ_{TM} cannot be the characteristic numbers, which is due to the impacts on the propagation speed of the thermal wave and its heat diffusion caused by the inertia term of the temperature gradient to time for the DPL model, and the inertia term of the temperature to time and nonlocal terms for the TM model, respectively. For the thermal waves predicted by the CV and simplified TM models, their propagation processes satisfy the exponential damping relationship in most situations, with the deviation occurring only when the overdamped cases play a major role and the thermal waves stay at the primary stage. Besides, the sharp and blunt thermal waves predict different slopes of $-\ln(1-\varepsilon_q)$ to the damping factor ξ. If the thermal wave is sharper, the overdamped cases are fewer, and therefore the corresponding slope of $-\ln(1-\varepsilon_q)$ to ξ is closer to 0.5. The studies are expected to help not only understand the thermal wave behaviours but also carry out experimental investigations and engineering evaluations.

1. Introduction

Heat conduction in solids is ordinarily considered as a diffusion phenomenon, which is generally described by the Fourier's law [1]. This is acceptable for normal engineering applications, but the non-physical infinite heat propagation speed assumption in the Fourier's law usually leads to its failure in situations such as high-power perturbation under short duration [2–4], ultralow temperature conditions [5,6], micro scale conditions [7–9], and biological tissues [10,11]. To remove this limitation, inertia of the heat flux, temperature and temperature gradient to time and nonlocal effects were introduced to modify the Fourier's law for achieving the heat propagation with finite speed [12–14], which further results in that the classical diffusive heat conduction process turns into a wave or ballistic phenomenon [15–18]. Several models have been pronounced for consideration of the non-Fourier effects [19,20], in which the typical ones are Cattaneo–Vernotte (CV) [21,22], dual-phase-lagging (DPL) [23–25], Guyer–Krumhansl (GK) [26,27], and thermomass (TM) models [28,29]. These models are, respectively, shown as follows:

$$q + \tau_q \frac{\partial q}{\partial t} = -k\nabla T, \tag{1}$$

$$q + \tau_q \frac{\partial q}{\partial t} = -k\left[\nabla T + \tau_T \frac{\partial}{\partial t}(\nabla T)\right], \tag{2}$$

* Corresponding author.
E-mail address: caoby@tsinghua.edu.cn (B.-Y. Cao).

http://dx.doi.org/10.1016/j.ijthermalsci.2014.04.014
1290-0729/

Nomenclature

A	wavelet's amplitude
C	arbitrary constants
C_v	specific heat, J/kg K
d	thickness, m
F	vector defined in Eq. (11)
i	imaginary number
k	thermal conductivity, W/m K
Kn	Knudsen number
l	mean free path, m
L	travelling distance, m
n	wave number, 1/m
q	heat flux, W/m^2
S	vector defined in Eq. (11)
t	time, s
T	temperature, K
ΔT	temperature, K
U	vector defined in Eq. (11)
W	vector defined in Eq. (13)
x	position, m
Z	dimensionless relaxation time

Greek symbols

α	thermal diffusivity, k/ρ C_v, m^2/s
γ	Grüneisen constant
ρ	density, kg/m^3
ξ	damping factor
ζ	damping ratio
τ	relaxation time, s
λ	wavelength, m
λ_j	eigenvalue, $j = 1, 2$
ε	damping level
v	propagation speed, m/s
ω	natural angular velocity, rad/s

Superscript

*	dimensionless parameter
q	heat flux
T	temperature

Subscript

0	initial temperature
CV	Cattaneo–Vernotte
DPL	dual-phase-lagging
f	frontier
f^0	reference frontier
g	phonon gas
N	normal process
p	peak
p0	peak corresponding to the reference frontier
q	heat flux
R	Umklapp process
T	temperature
TM	thermomass
TM0	thermomass at initial temperature
v	volume
w	thermal wave

$$q + \tau_R \frac{\partial q}{\partial t} = -\frac{v_g^2 \tau_R C_v}{3}\nabla T + \frac{\tau_R \tau_N v_g^2}{5}\left[\nabla^2 q + 2\nabla(\nabla\cdot q)\right], \tag{3}$$

$$q + \tau_{TM}\frac{\partial q}{\partial t} - \tau_{TM}\frac{q}{T}\frac{\partial T}{\partial t} + \tau_{TM}\frac{q}{\rho C_v T}\nabla\cdot q - \tau_{TM}\frac{q}{\rho C_v T}\cdot\frac{q}{T}\nabla T = -k\nabla T. \tag{4}$$

In Eqs. (1)–(4), q is the heat flux, T is the temperature, t is the time, k is the thermal conductivity, ρ is the mass density, and C_v is the heat capacity at constant volume. The relaxation time of heat flux τ_q in the CV and DPL models are both based on the consideration of phonon collisions and defined as the ratio of the mean free path (l) of phonons to their group speed (v_g) [30]. The relaxation time of the temperature gradient τ_T in the DPL model is based on the consideration of the micro-structural interactions [31]. The relaxation times τ_R and τ_N in the GK model describe the Umklapp (momentum non-conserving) and normal (momentum conserving) processes in the phonon interactions [32], and the term $\frac{\tau_R \tau_N v_g^2}{5}[\nabla^2 q + 2\nabla(\nabla\cdot q)]$ is due to the second-order nonlocal effect. The characteristic time τ_{TM} in the TM model is $k/(2\gamma\rho C_v^2 T)$ [18], where γ is the Grüneisen constant. The different expression of the characteristic time in the TM model is because this model is established by accommodating the equivalent mass of phonon gas calculated from the Einstein mass–energy equation and using the mass and momentum conservation equations for the weighty and compressible phonon gas.

The CV model can be reduced to the Fourier's law when τ_q is negligible, or the thermal perturbation is weak. If we neglect the inertia term of the temperature and temperature gradient to time and nonlocal effects, the DPL, GK, and TM model can all turn into the CV model. However, these models may predict different heat propagation behaviours. The heat propagation process predicted by the DPL model is determined by the relative sizes between τ_q and τ_T, and this model actually includes four heat propagation modes: wavy mode ($\tau_T = 0$), wavelike mode ($0 < \tau_T < \tau_q$), diffusion mode ($\tau_T = \tau_q$), and over-diffusion mode ($\tau_T > \tau_q$) [33]. Due to the nonlocal effect, the resulting thermal wave predicted by the GK model propagates faster than that predicted by the CV model and the temperature level in the affected region is much higher [32]. For the TM model, it agrees well with the CV model when the thermal perturbation and heat flux are sufficiently weak [34]. But for the large thermal perturbation, the CV model may predict unphysical negative temperature when two cooling thermal waves superpose, and this limitation could be overcome by the TM model [34,35].

From the CV, DPL, GK, and TM models, it can be seen that these models all include the diffusion (q) and wave ($\tau(\partial q/\partial t)$) terms, where τ are τ_q, τ_q, τ_R, τ_{TM}, respectively. So, due to the effect of the heat diffusion, the energy transported by the thermal waves predicted by these models will reduce gradually, which further gives rise to the damping of the thermal perturbations. Tang and Araki [36] studied the wavy, wavelike, and diffusive thermal responses, predicted by the DPL model, in finite rigid slabs under pulse surface heating and obtained analytical temperature distributions using the Green's function method. The results showed that for wavy mode, namely the CV model, increasing the propagation process only leads to the damping of the temperature amplitude while not any change in the wide of the portion of the thermal wave, but for the wavelike mode, the propagation will lead to both the damping of the temperature amplitude and the dissipation of the portion of the thermal wave. As for the damping of the temperature wave predicted by the CV model, Ramadan [37] declared that the reason is the damping effect of the heat diffusion. Jou et al. [38] further pointed out that for the CV model, if neglecting the diffusion term, the temperature wave will not change during its propagation

process; but if retaining the diffusion term, the temperature amplitude will decrease gradually. For the GK and TM models, Tzou [32] and Lam [39] also reported respectively that the temperature amplitude reduced with the temperature wave moving forward.

Although the damping of the thermal waves predicted by the CV, DPL, GK, and TM models has been confirmed by many researchers, quantitative studies on this topic remain seldom thus far. Moreover, Lor and Chu [40] found that the temperature and heat flux waves both appear in this process, but until now, there is no report giving out that the damping of which one can reflect the damping behaviour better. In a sum, for the damping of the thermal waves, the key problem is the lack of specific factors that can determine and evaluate this process and the corresponding theoretical analysis for these factors. Undoubtedly, these factors are particularly important to the experimental investigations on the non-Fourier effect because we can predict the amplitude of the thermal perturbation in advance. So, studies on the damping of thermal waves can not only help us understand this process better, but also help us carry out experimental investigations and engineering evaluations.

In this paper, we proposed the damping factor and damping levels of the temperature and heat flux for studying the damping of the thermal waves, which will be shown in Section 3. The verified numerical methods were adopted to test the effectiveness of these numbers. Further, considering the similarity between the damping of the thermal waves and damped oscillations, we carried out theoretical studies on this process using the damped vibration theory and gave out the limitation of these numbers.

2. Numerical method and its validation

To study the damping of the thermal waves quantitatively, we consider a one-dimensional heat conduction problem in a finite rigid slab under surface heat flux pulse heating. Since the DPL model is similar to the GK model for the one-dimensional problem [19], we only discuss the damping of the thermal waves predicted by the CV, DPL, and TM models. The one-dimensional CV, DPL and TM models are, respectively, shown as below:

$$q+\tau_{\mathrm{q}}\frac{\partial q}{\partial t}=-k\frac{\partial T}{\partial x}, \tag{5}$$

$$q+\tau_{\mathrm{q}}\frac{\partial q}{\partial t}=-k\left(\frac{\partial T}{\partial x}+\tau_{\mathrm{T}}\frac{\partial^2 T}{\partial x\partial t}\right), \tag{6}$$

$$q+\tau_{\mathrm{TM}}\frac{\partial q}{\partial t}-\tau_{\mathrm{TM}}\frac{q}{T}\frac{\partial T}{\partial t}+\tau_{\mathrm{TM}}\frac{q}{\rho C_{\mathrm{v}}T}\frac{\partial q}{\partial x}-\tau_{\mathrm{TM}}\frac{q}{\rho C_{\mathrm{v}}T}\cdot\frac{q}{T}\frac{\partial T}{\partial x}=-k\frac{\partial T}{\partial x}. \tag{7}$$

To obtain the temperature and heat flux distributions predicted by these models, we also need the energy conservation equation, given as follows:

$$\rho C_{\mathrm{v}}\frac{\partial T}{\partial t}+\frac{\partial q}{\partial x}=0. \tag{8}$$

Considering the analytical solutions only apply to the simple initial boundary conditions, the high-order purely numerical explicit total-variation-diminishing (TVD) scheme with Roe's superbee limiter function was adopted in this paper. This numerical method was first established by Yang [41]. Shen and Zhang used it for calculating the temperature and heat flux distributions predicted by the CV and DPL models and its effectiveness for this was confirmed [42]. The numerical method used in this paper is the same with that used by Shen and Zhang [42] with the only difference of the normalization method of the temperature. The numerical diffusion exists in the sharp temperature and heat flux edges when using this numerical method [41]. But to make the effects of the numerical diffusion can be neglected and ensure the independence of the calculated grids, enough uniform calculated grids are chosen in this paper. We use the DPL model for introduction of the TVD scheme. This is because the CV model can use this scheme by setting τ_{T} in the DPL model as 0 and the TM model can use this scheme through replacing the term $\tau_{\mathrm{T}}(\partial^2 T/\partial x\partial t)$ in the DPL model by the inertia term of the temperature to time and nonlocal terms of the temperature and heat flux in the TM model. Before presenting the TVD scheme for the DPL model, we should define the dimensionless position x^*, time t^*, temperature T^*, heat flux q^*, characteristic times Z_{q} and Z_{T}, which are, respectively, shown as follows:

$$\begin{aligned} &x^*=x/d,\ t^*=t\Big/\left(d^2\Big/\alpha\right),\ T^*=T/T_0,\ q^*=q/(kT_0/d),\\ &Z_{\mathrm{q}}=\tau_q\Big/\left(d^2\Big/\alpha\right),\ Z_{\mathrm{T}}=\tau_T\Big/\left(d^2\Big/\alpha\right), \end{aligned} \tag{9}$$

where d is the thickness of the slab and α is its thermal diffusivity, defined as $k/(\rho C_{\mathrm{v}})$.

Then, using the normalization method defined in Eq. (9), the DPL model in Eq. (6) and energy conservation equation in Eq. (8) can be transformed into the dimensionless vector form as:

$$\frac{\partial \boldsymbol{U}}{\partial t^*}+\frac{\partial \boldsymbol{F}}{\partial x^*}=\boldsymbol{S}, \tag{10}$$

with the vectors defined as:

$$\boldsymbol{U}=\begin{bmatrix} Z_{\mathrm{q}}q^* \\ T^* \end{bmatrix},\ \boldsymbol{F}=\begin{bmatrix} T^* \\ q^* \end{bmatrix},\ \boldsymbol{S}=\begin{bmatrix} -q^*-Z_{\mathrm{T}}\dfrac{\partial^2 T^*}{\partial x^*\partial t^*} \\ 0 \end{bmatrix}. \tag{11}$$

Further, following the steps of diagonalization based on eigenvalue presented in [41], we can rewrite the dimensionless vector equation in Eq. (10) into two separately independent equations:

$$\frac{\partial W_j}{\partial t^*}+\lambda_j\frac{\partial W_j}{\partial x^*}=S_j,\ j=1,2, \tag{12}$$

where

$$\begin{aligned} &\begin{bmatrix} W_1 \\ W_2 \end{bmatrix}=\begin{bmatrix} \dfrac{1}{2}\left(T^*+\sqrt{Z_{\mathrm{q}}}q^*\right) \\ \dfrac{1}{2}\left(T^*+\sqrt{Z_{\mathrm{q}}}q^*\right) \end{bmatrix},\ \begin{bmatrix} \lambda_1 \\ \lambda_2 \end{bmatrix}=\begin{bmatrix} \dfrac{1}{\sqrt{Z_{\mathrm{q}}}} \\ -\dfrac{1}{\sqrt{Z_{\mathrm{q}}}} \end{bmatrix},\\ &\begin{bmatrix} S_1 \\ S_2 \end{bmatrix}=\begin{bmatrix} -\dfrac{1}{2\sqrt{Z_{\mathrm{q}}}}\left(q^*+Z_{\mathrm{T}}\dfrac{\partial^2 T^*}{\partial x^*\partial t^*}\right) \\ \dfrac{1}{2\sqrt{Z_{\mathrm{q}}}}\left(q^*+Z_{\mathrm{T}}\dfrac{\partial^2 T^*}{\partial x^*\partial t^*}\right) \end{bmatrix}. \end{aligned} \tag{13}$$

Eventually, the equations in Eq. (12) can be readily solved by the TVD scheme with the Roe's superbee limiter function, the detail of which can be acquired in Ref. [41].

After establishing the TVD scheme for obtaining the temperature and heat flux distributions, we should testify its effectiveness. The one-dimensional heat conduction problem such as one thin slab under surface heat flux heating reported by Shen and Zhang [42] was taken for the validation of the numerical method used in this paper. Here, the thin slab is finite in the x-direction while infinite in the y- and z-directions. The

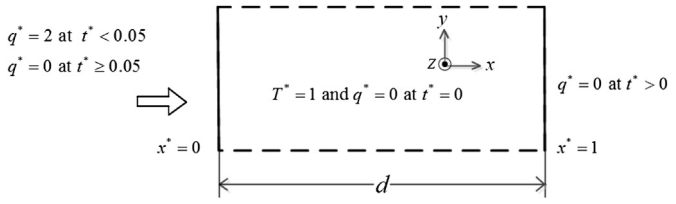

Fig. 1. Schematic diagram for a one-dimensional heat conduction problem under surface heat flux pulse heating.

corresponding schematic diagram for this problem is shown in Fig. 1 with the initial boundary conditions defined in Eqs. (14)–(16).

$$T^* = 1 \text{ and } q^* = 0 \text{ at } t^* = 0, \tag{14}$$

$$q^* = 2 \text{ at } x^* = 0,\ t^* < 0.05 \text{ and } q^* = 0 \text{ at } x^* = 0,\ t^* \geq 0.05, \tag{15}$$

$$q^* = 0 \text{ at } x^* = 1,\ t^* > 0. \tag{16}$$

Fig. 2 presents the comparisons between the spatial dimensionless temperature and heat flux distributions at $t^* = 0.4$ predicted by the CV and DPL models in our work and the numerical solutions in Ref. [42]. From Fig. 2, it can be easily seen that for both the CV and DPL models, the predicted numerical solutions in our work agree well with those in Ref. [42]. Since we can rewrite the formulation of the TM model to adjust the TVD scheme established for the DPL model, this scheme can also be effective for calculating the temperature and heat flux distributions predicted by the TM model. So, after the validation, it can be concluded that the numerical method established in this paper can be used for the studies on the damping of the thermal waves.

3. Physical problem

When studying the damping of the thermal waves predicted by the CV, DPL and TM models, we reconsider the one-dimensional heat conduction problem in Fig. 1 with the initial boundary conditions defined in Eqs. (14)–(16), but in which we replaced the constant heat flux pulse in Eq. (15) by a cosine heat flux pulse, taking the form as:

$$q = [1 - \cos(2\pi t/0.05)] \text{ at } x = 0,\ t < 0.05 \text{ and } q = 0 \text{ at } x = 0,\ t \geq 0.05, \tag{17}$$

which is also normalized using the method defined in Eq. (9). Besides, we define a series of base conditions for the CV, DPL, and TM models, as shown in Table 1. Here, x^*_{f0} represents the dimensionless reference frontier position of the temperature and heat flux wave, and L represents the travelling distance of the temperature and heat flux wave. The reason why we let reference frontier position be near a specific position is that it is hard to determine the speed of the thermal waves predicted by the DPL and TM models, and more importantly, the different choices of x^*_{f0} will not affect the conclusions in this paper.

To understand the damping of the thermal waves better, we take the CV model under base condition CV-1 for example and obtain the propagation processes of the temperature and heat flux wave using the TVD scheme established above. The spatial dimensionless temperature and heat flux distributions at different dimensionless wave frontier positions x^*_f predicted by the CV model are shown in Fig. 3. From Fig. 3, we can know that for the CV model, the heat propagation process is indeed in a wave mode with the temperature and heat flux of some inner regions exceeding those at the boundary. With the temperature and heat flux waves moving forward, their amplitudes both decrease continuously due to the heat diffusion. Although the thermal perturbation is strong when $x^*_f = 0.1$, it becomes quite weak when $x^*_f = 0.9$. The strong heat diffusion can result in such significant attenuation of the signals of the temperature and heat flux waves that we cannot capture them after travelling quite long distances.

It should be mentioned that the dimensionless temperature and heat flux distributions could be greatly affected by the boundary conditions. In Fig. 1, we adopted the boundary conditions: first heat flux pulse heating and then adiabatic are imposed at $x^* = 0$ and always adiabatic at $x^* = 1$. The corresponding dimensionless temperature and heat flux distributions are shown in Fig. 3. The dimensionless temperature and heat flux distributions both have peak values with the sharp wavefront and wavebehind. But, if significantly increasing the heat pulse duration, the peak values will weaken and even may not appear due to slower time variation of the heat flux. If greatly decreasing the relaxation time τ_q in the CV model, the peak values may also be not observed at the computing instants of time in this paper due to the stronger damping of the thermal waves discussed in Section 4.1. Besides, the propagation process of the thermal waves can also be affected by the boundary condition on the right hand, which can affect the

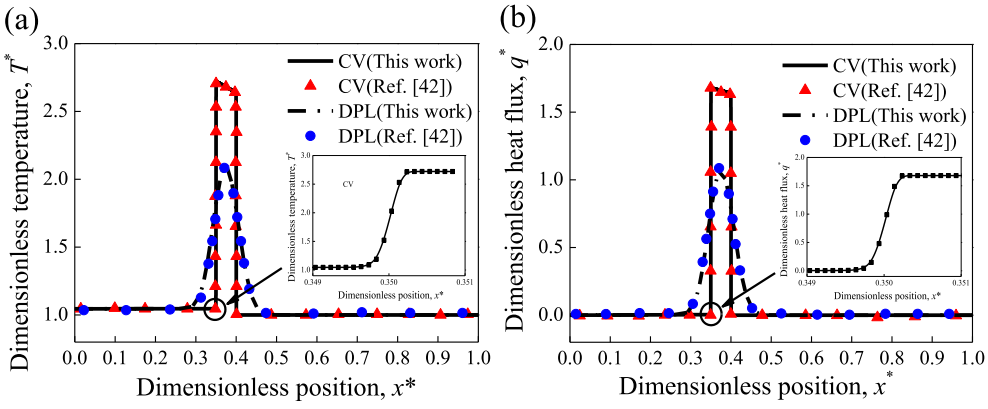

Fig. 2. Comparisons between the spatial dimensionless temperature and heat flux distributions at $t^* = 0.4$ predicted by the CV and DPL models in this work and the numerical solutions in Ref. [42].

Table 1
Base conditions for the CV, DPL, and TM models.

	k	ρ	C_v	T_0	d	τ_q	τ_T	γ	x^*_{f0}	L
CV-1	0.1	1.0	1.0	1.0	1.0	0.2	–	–	0.2	0.7d
DPL-1	0.1	1.0	1.0	1.0	1.0	0.2	0.002	–	Near 0.2	0.7d
TM-1	1.0	20.0	1.0	1.0	1.0	–	–	0.1	0.2	0.7d
TM-2	1.0	20.0	1.0	1.0	1.0	–	–	0.1	Near 0.2	0.7d

reflection of the temperature and heat flux waves. When using the constant temperature boundary condition on the right hand instead of the adiabatic right boundary condition, the temperature and heat flux waves after reflected by the right side are exactly that the temperature and heat flux waves turn upside down at the same instant of time when using the adiabatic boundary condition on the right hand [42]. If using the temperature pulse boundary condition, such as making the temperature at $x^* = 0$ having a sudden increase and then keeping this temperature [14], the thermal waves can only have sharp wavefront and does not have sharp wavebehind. Although the boundary condition can affect the temperature and heat flux waves, the damping of the thermal waves always exists in their propagation processes. To facilitate our quantitative study, we adopt the boundary conditions: first heat flux pulse and then adiabatic are imposed at $x^* = 0$ while always adiabatic at $x^* = 1$, as shown in Eq. (17).

For quantitative studies on the damping of thermal waves, it is quite necessary to define specific factors that can evaluate and determine this process. Since it is relatively easier to find factors used for evaluating the damping of the thermal waves, we first define the damping levels of the temperature and heat flux waves for evaluation, given as below:

$$\varepsilon_T = \frac{T\left(x^T_{p0}\right) - T\left(x^T_{p0} + L\right)}{T\left(x^T_{p0}\right)}, \tag{18}$$

$$\varepsilon_q = \frac{q\left(x^q_{p0}\right) - q\left(x^q_{p0} + L\right)}{q\left(x^q_{p0}\right)}. \tag{19}$$

Here, ε_T and ε_q are the damping levels of the temperature and heat flux wave, respectively. x^T_{p0} and x^q_{p0} are the positions of the temperature and heat flux peaks when the dimensionless frontier positions of the temperature and heat flux waves both reach the dimensionless reference position x^*_{f0}, respectively. $T(x)$ and $q(x)$ are the temperature and heat flux at the position x, respectively, in which x can be x^T_{p0}, x^q_{p0}, $(x^T_{p0} + L)$, $(x^q_{p0} + L)$. So, $T(x^T_{p0})$ and $q(x^q_{p0})$ are actually the amplitudes of the temperature and heat flux waves when their frontier positions reach x^*_{f0}, respectively. $T(x^T_{p0} + L)$ and $x^q_{p0} + L$ are the amplitudes of the temperature and heat flux waves after their peaks travelling the distance L relative to x^T_{p0} and x^q_{p0}, respectively.

After defining the damping levels of the temperature and heat flux waves, we need to find a specific factor that can determine the damping of the thermal waves. This factor is better to serve as a characteristic number, which has decisive impact on this process. For this, we got an idea from the dimensionless relaxation time $Z_q = \tau_q/(d^2/\alpha)$ and proposed a new dimensionless factor

$$\xi = L/\sqrt{\alpha\tau}, \tag{20}$$

where τ is τ_q for the CV and DPL models, or τ_{TM} for the TM model. As ξ is directly used for determining the damping of the thermal waves, we can call it the damping factor. Why we chose the damping factor ξ for controlling the damping process comes from two considerations. Taking the CV model for example, one consideration is that we can substitute $v_w = \sqrt{\alpha/\tau}$, where v_w is the speed of the thermal wave predicted by the CV model, into Eq. (20) and reformulate ξ as

$$\xi = \frac{L}{v_w\tau}. \tag{21}$$

As we know, increasing the travelling distance L, decreasing the wave speed v_w, or decreasing the relaxation time τ means that the thermal wave needs more time to travel the distance L at the wave speed v_w, or the impact of the wave term relative to the heat diffusion term decreases. These changes all can lead to the increase of the damping extent of the energy transported by the thermal wave and at the same time, they also leads to the increase of the damping factor ξ. So, no matter which change leads to the increase of ξ, if ξ increases, the damping extent of the energy transported by the thermal wave increases, and vice versa. The other consideration is that we can substitute

$$\alpha = \frac{k}{\rho C_v} = \frac{\rho C_v v_g l/3}{\rho C_v} = \frac{v_g l}{3}, \tag{22}$$

where l is the mean free path of phonons and v_g is their group speed [43], into Eq. (20) and rewrite ξ as

$$\xi = \frac{\sqrt{3}L}{\sqrt{v_g\tau l}}. \tag{23}$$

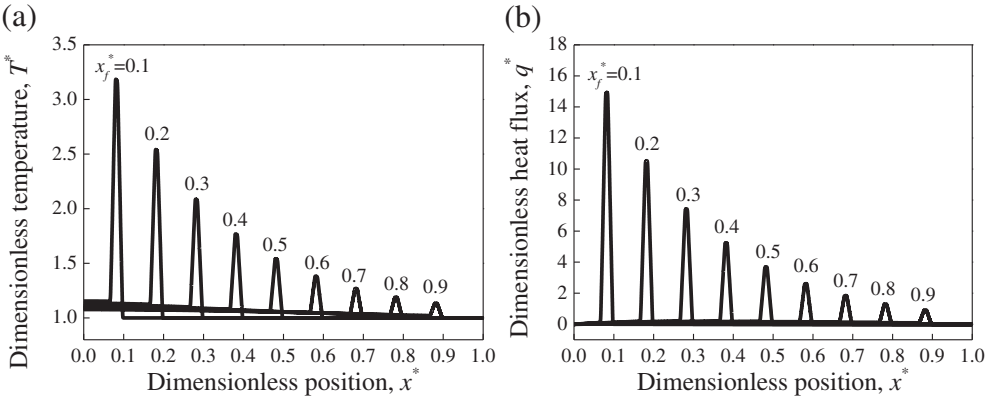

Fig. 3. The spatial dimensionless temperature and heat flux distributions at different dimensionless wave frontier positions predicted by the CV model.

Considering $v_g\tau = l$ and $l/L = Kn$, where Kn is the Knudsen number, we can reformulate Eq. (23) as

$$\xi = \frac{\sqrt{3}}{Kn}. \tag{24}$$

The decrease of Kn means stronger collisions between/among phonons, namely stronger heat diffusion and quicker damping of the energy transported by the thermal wave. So, from the view of Kn, we can also know if the damping factor ξ increases, the damping extent of the energy transported by the thermal wave increases, and vice versa. From the above two considerations, we determine the expression of the damping factor ξ. For the wavelike mode of the DPL model considered in this paper, the introduction of τ_T leads to faster heat propagation speed and stronger heat diffusion. But it is hard to determine the effects of τ_T on the damping of the thermal waves quantitatively now, and therefore we do not consider the effects of τ_T here and still use $L/\sqrt{\alpha\tau_q}$ as the damping factor for the DPL model. For the TM model, it is also hard to predict the effects of the inertia term of the temperature to time and nonlocal effects on the damping of the thermal waves quantitatively now, and thus we adopt the same strategy for the DPL model and use $L/\sqrt{\alpha\tau_{TM}}$ as the damping factor for the TM model.

In summary, the damping levels of the temperature and heat flux ε_T and ε_q defined in Eqs. (18) and (19) are used for evaluating of the damping extent of the thermal waves while the damping factors defined for the thermal waves predicted by the CV, DPL, and TM models are used for determining their damping extent. The thermal properties of the slab and travelling distances of the thermal waves can all affect the damping factors. But, the damping levels of the temperature and heat flux are defined directly from the peak signals of the temperature and heat flux waves. The damping factors can be used for predicting the damping extent of the thermal waves, but the damping levels are only the indictors which are used for evaluating their damping extent.

4. Results and discussion

4.1. CV model

Using the base condition CV-1, we obtained the effects of the damping factor ξ_{CV} $(L/\sqrt{\alpha\tau_q})$ on the damping levels of the temperature and heat flux predicted by the CV model, as shown in Fig. 4. Here, the damping factors are varied due to the changes of L, τ_q, k, ρ and C_v, respectively. Besides, if one of L, τ_q, k, ρ and C_v changes, we assume the others do not change. From Fig. 4, it can be seen that effects of the damping factor ξ_{CV} due to the changes of L, τ_q, k, ρ and C_v separately on the damping level of the heat flux ε_q predicted by the CV model overlap together while those on the damping level of the temperature ε_T do not. This is because the heat flux is directly related to the energy transported by the thermal wave, but the temperature also can be affected by the thermal properties of the slab. For the damping level of the heat flux, no matter how L, τ_q, k, ρ or C_v changes, if the damping factor ξ_{CV} increases, more energy transported by the thermal wave is diffused. Therefore, the damping level of the heat flux predicted by the CV model increases with the damping factor ξ_{CV} increasing. But for the damping level of the temperature, the increase of the damping factor ξ_{CV} may be caused by the increase of L, ρ and C_v, the decrease of τ_q and k, or their combined impacts. If considering $T = T_0 + \Delta T$, the damping level of the temperature ε_T in Eq. (18) can be reformulated into

$$\varepsilon_T = \frac{\Delta T\left(x_{p0}^T\right) - \Delta T\left(x_{p0}^T + L\right)}{T_0 + \Delta T\left(x_{p0}^T\right)}. \tag{25}$$

Further, Eq. (25) can rewritten as

$$\varepsilon_T = \left(1 - \frac{T_0}{T_0 + \Delta T\left(x_{p0}^T\right)}\right) \frac{\Delta T\left(x_{p0}^T\right) - \Delta T\left(x_{p0}^T + L\right)}{\Delta T\left(x_{p0}^T\right)}. \tag{26}$$

As the local temperature increase is in direct proportion to the local heat flux, the damping level of the temperature ε_T obey the relationship:

$$\varepsilon_T \propto \left(1 - \frac{T_0}{T_0 + \Delta T\left(x_{p0}^T\right)}\right) \frac{q\left(x_{p0}^q\right) - q\left(x_{p0}^q + L\right)}{q\left(x_{p0}^q\right)}, \tag{27}$$

which also can be reformulated into

$$\varepsilon_T \propto \left(1 - \frac{1}{1 + \Delta T^*\left(x_{p0}^T\right)}\right) \varepsilon_q, \tag{28}$$

where $\Delta T^*(x_{p0}^T) = \Delta T(x_{p0}^T)/T_0$. The increase of L, ρ and C_v and the decrease of τ_q and k all can lead to the increase of ε_q, but the increase of L does not change $\Delta T^*(x_{p0}^T)$, the increase of ρ and C_v and the decrease of τ_q result in the decrease of $\Delta T^*(x_{p0}^T)$ while the decrease of k results in the increase of $\Delta T^*(x_{p0}^T)$. So, from Eq. (28), we can know if the damping factor ξ_{CV} increases due to the increase of L or the decrease of k, the damping level of temperature predicted by the CV model always increases. But if the damping factor increases due to the increase of ρ and C_v and the decrease of τ_q, $(1 - (1/(1 + \Delta T^*(x_{p0}^T))))$ increases while ε_q decreases. When the damping factor is relatively small, the impact of $(1 - (1/(1 + \Delta T^*(x_{p0}^T))))$ is stronger than that of ε_q, and therefore the damping level of the temperature increases first. But when the damping factor increases to a specific value, the impact of ε_q begin to take a major role, and then the damping level of the temperature decreases. Besides, we can find that effects of the damping factor due the changes of ρ and C_v on the damping level of the temperature overlap together, which is due to the impact of ρ and C_v on the temperature increase is same.

After the above discussion, we can know for evaluating the damping of the thermal wave predicted by the CV model, the damping level of the heat flux ε_q is a better factor than that of the temperature. Under the base condition CV-1, effects of the damping factor due to the changes of L, τ_q, k, ρ and C_v separately on the damping level of the heat flux overlap together show that the damping factor ξ_{CV} can be a characteristic number for determining the damping of the thermal wave predicted by the CV model. Besides, it should be particularly mentioned that the above conclusions also hold if the reference positions x_{p0}^T and x_{p0}^q change.

4.2. DPL model

Using the base condition DPL-1, we obtained the effects of the damping factor ξ_{DPL} $(L/\sqrt{\alpha\tau_q})$ on the damping levels of the temperature and heat flux predicted by the DPL model, as shown in Fig. 5. Here, the damping factors are varied due to the changes of L, τ_q, k, ρ and C_v, respectively. Besides, if one of L, τ_q, k, ρ and C_v changes, we also assume the others do not change. The only difference between the base conditions CV-1 and DPL-1 is the relaxation time τ_T. If neglecting the relaxation time τ_T, the DPL model will turn into the CV model, and corresponding effects of the damping factor ξ_{DPL} due to the changes of L, τ_q, k, ρ or C_v on the damping level of the heat flux will overlap together. But from Fig. 5, we can find that the effects of the damping factor ξ_{DPL} due to the changes of L, τ_q, k, ρ and C_v separately on the damping level of the heat flux

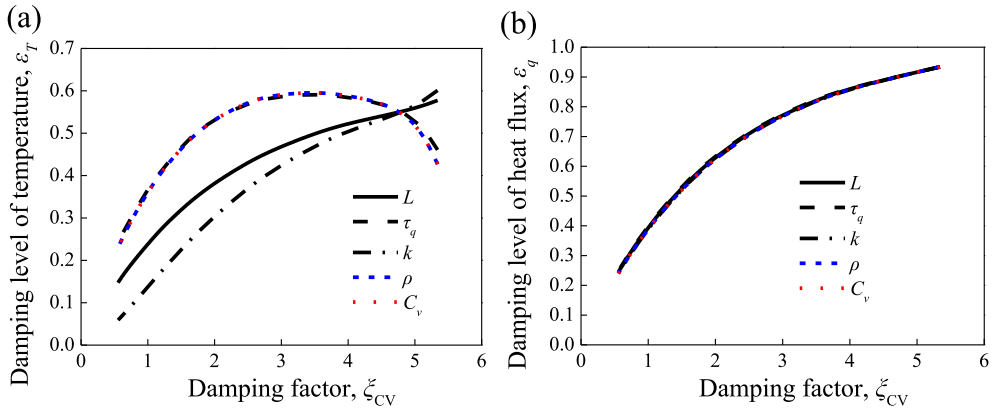

Fig. 4. Effects of the damping factor ξ_{CV} on the damping levels of the (a) temperature and (b) heat flux predicted by the CV model, in which the damping factors are varied due to the changes of L, τ_q, k, ρ and C_v, respectively.

predicted by the DPL model do not overlap together. This is due to the impact of the relaxation time τ_T, which increases both the speed of the thermal wave and heat diffusion. This further results in that the damping factor ξ_{DPL} cannot be a characteristic number for the DPL model, especially when ξ_{DPL} is relatively small, namely the heat diffusion is weak. When ξ_{DPL} is quite large, the common strong heat diffusion under these conditions makes that effects of the damping factor on the damping level of the heat flux overlap together. Besides, the variation trends of the damping levels of temperature and heat flux predicted by the DPL model with the damping factor ξ_{DPL} are same with those predicted by the CV model. The increase of the damping factor ξ_{DPL} due to the increase of L or the decrease of k lead to the increase of the damping level of the temperature, but that due to the increase of ρ and C_v, or the decrease of τ_q will lead to the first increase and then decrease of the damping level of the heat flux. The increase of the damping factor ξ_{DPL} due to these changes all result in the increase of the damping level of the heat flux predicted by the DPL model.

So, for the damping of the thermal wave predicted by the DPL model, the damping level of the heat flux ε_q is a better factor than that of the temperature. This is same with that of the CV model because the heat flux is directly related to the energy transported by the thermal wave while the temperature can also be affected by the thermal properties. But, as the damping factor ξ_{DPL} $(L/\sqrt{\alpha\tau_q})$ does not consider the impacts of the relaxation time τ_T, it cannot be the characteristic number for determining the damping of the thermal wave predicted by the DPL model, especially when τ_T is relatively large. Considering there is no effective method to determine the impact of τ_T on the speed of the thermal wave predicted by the DPL model and its heat diffusion quantitatively currently, the more appropriate definition of the damping factor for the DPL model considering the impacts of τ_T needs further studies.

4.3. TM model

The TM model includes not only the inertia term of heat flux to time, but also the inertia term of the temperature to time and nonlocal effects of the temperature and heat flux. To facilitate the studies, we can first neglect the inertia term of the temperature to time and nonlocal terms and only retain the inertia term of the heat flux to time. The corresponding TM model in Eq. (7) turns into

$$q + \tau_{TM}\frac{\partial q}{\partial t} = -k\frac{\partial T}{\partial x}. \tag{29}$$

As the relaxation time τ_{TM} is a function of the local temperature and the local temperatures that the thermal wave passes are varied, the damping factors are also varied, and hence it's very difficult to determine the synthetic damping factor for the whole process. Besides, Zhang et al. [44] reported that if considering the case that the relaxation time τ_{TM} decreases with the temperature increasing, the thermal wave predicted by the TM model will propagate faster in regions with higher temperature, and therefore the dispersion phenomenon will occur. Under this situation, many peaks of the temperature will appear in the propagation process of the thermal

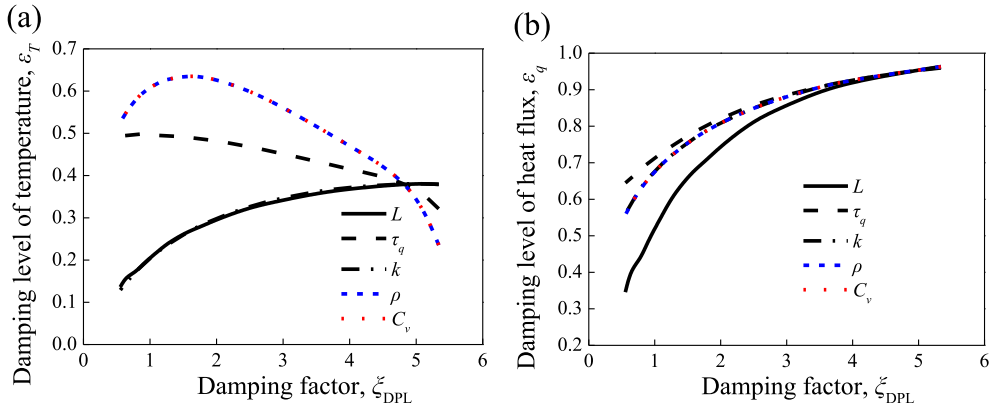

Fig. 5. Effects of the damping factor ξ_{DPL} on the damping levels of the (a) temperature and (b) heat flux predicted by the DPL model, in which the damping factors are varied due to the changes of L, τ_q, k, ρ and C_v, respectively.

wave, hence it's more difficult to determine the damping levels of the temperature and heat flux, and the corresponding damping factor. For the convenience of the test of the damping levels of the temperature and heat flux and the damping factor, we can consider the situation that the temperature increase is quite small. So, through assuming that the temperature in the relaxation time τ_{TM} is the initial temperature T_0, the TM model in Eq. (29) becomes

$$q + \tau_{TM0}\frac{\partial q}{\partial t} = -k\frac{\partial T}{\partial x}, \tag{30}$$

where $\tau_{TM0} = k/(2\gamma\rho C_v^2 T_0)$. So, the simplified TM model in Eq. (30) is similar to the CV model with the only difference of the relaxation time. If changing the mass density ρ, thermal conductivity k and heat capacity C_v, the relaxation time τ_q in the CV model is constant while the characteristic time τ_{TM0} in the simplified TM model changes accordingly.

Using the base condition TM-1, we obtained the effects of the damping factor ξ_{TM0} $(L/\sqrt{\alpha\tau_{TM0}})$ on the damping levels of the temperature and heat flux predicted by the simplified TM model in Eq. (30), as shown in Fig. 6. Here, the damping factors are varied due to the changes of L, γ, k, ρ and C_v, respectively. Besides, if one of L, γ, k, ρ and C_v changes, we assume the others do not change. From Fig. 6, it can be found that similar to the CV model, effects of the damping factor ξ_{TM0} due to the changes of L, γ, k, ρ and C_v separately on the damping level of the heat flux ε_q predicted by the simplified TM model overlap together while those on the damping level of temperature ε_T do not. The increase of the damping factor ξ_{TM0} due to the changes of L, γ, k, ρ or C_v all can result in more energy transported by the thermal wave diffused after travelling the distance L, and hence the damping level of the heat flux predicted by the simplified TM model also increase with the damping factor ξ_{TM0}. So, the variation trends of the damping level of the heat flux predicted by the simplified TM model with the damping factor ξ_{TM0} are same with the CV and DPL models. But for the damping level of the temperature predicted by the simplified TM model, its variation trends with k, ρ and C_v is different from those predicted by the CV model. Unlike that the decrease of k leads to the increase of $\Delta T^*(x_{p0}^T)$ predicted by the CV model, the decrease of k can lead to the decrease of $\Delta T^*(x_{f0})$ predicted by the simplified TM model, which is due to the increase of the relaxation time τ_{TM0}. So, with the damping factor ξ_{TM0} increasing due to the decrease of k, the increase of ε_q first takes a major role and then the decrease of $(1-(1/(1+\Delta T^*(x_{p0}^T))))$ takes a major role, which further resulting in that the damping level of the temperature first increases and then decrease. The increase of γ, ρ or C_v all can lead to the increase of the damping factor ξ_{TM0} and the decrease of $\Delta T^*(x_{p0}^T)$. Under the present situations, the decrease of $(1-(1/(1+\Delta T^*(x_{p0}^T))))$ takes a major role when γ, ρ or C_v increases, and therefore the damping level of temperature decreases with the increase of the damping factor ξ_{TM0} due to the changes of γ, ρ or C_v. Besides, it can be found that the effects of the damping factor ξ_{TM0} on the damping level of the temperature predicted by the simplified TM model do not overlap together. This is because that although the impacts of ρ and C_v on the temperature increase are same, they do not have the same impact on the relaxation time τ_{TM0}. Since $\Delta T^*(x_{p0}^T)$ does not change when L increases, the damping level of the temperature increases with L increasing.

After the above discussion, we can know for evaluating the damping of the thermal wave predicted by the simplified TM model in Eq. (29), the damping level of the heat flux ε_q is a better factor than that of the temperature. Under the base condition TM-1, effects of the damping factor due to the changes of L, γ, k, ρ and C_v separately on the damping level of the heat flux overlap together show that the damping factor ξ_{TM} $(L/\sqrt{\alpha\tau_{TM}})$ can be a characteristic number for determining the damping of the thermal wave predicted by the simplified TM model in Eq. (29). Besides, it should be particularly mentioned that the reference positions x_{p0}^T and x_{p0}^q do not affect the above conclusions.

Further, if considering the inertia term of the temperature to time and nonlocal effects of the temperature and heat flux, we need to test whether the damping factor ξ_{TM} $(L/\sqrt{\alpha\tau_{TM}})$ applies to the TM model in Eq. (7). Also considering the situation the temperature increase is quite small and only assuming the temperature in the relaxation time τ_{TM} of the inertia term of the heat flux to time is the initial temperature T_0, the TM model in Eq. (7) can be transformed into

$$q+\tau_{TM0}\frac{\partial q}{\partial t}-\tau_{TM}\frac{q}{T}\frac{\partial T}{\partial t}+\tau_{TM}\frac{q}{\rho C_v T}\frac{\partial q}{\partial x}-\tau_{TM}\frac{q}{\rho C_v T}\cdot\frac{q}{T}\frac{\partial T}{\partial x}=-k\frac{\partial T}{\partial x}. \tag{31}$$

Using the base condition TM-2, we obtained effects of the damping factor ξ_{TM0} $(L/\sqrt{\alpha\tau_{TM0}})$ on the damping levels of the temperature and heat flux predicted by the simplified TM model in Eq. (30), as shown in Fig. 7. Here, the damping factors are varied due to the changes of L, γ, k, ρ and C_v, respectively. Besides, if one of L, γ, k, ρ and C_v changes, we assume the others do not change. From Fig. 7, it can be found that unlike that for the simplified TM model in Eq. (30), effects of the damping factor ξ_{TM0} due to the changes of L, γ, k, ρ and C_v separately on the damping level of the heat flux do not overlap together. This is due to the impacts of the inertia term of the temperature to time and nonlocal terms on the speed of the thermal wave predicted by the TM model as well as the heat diffusion in

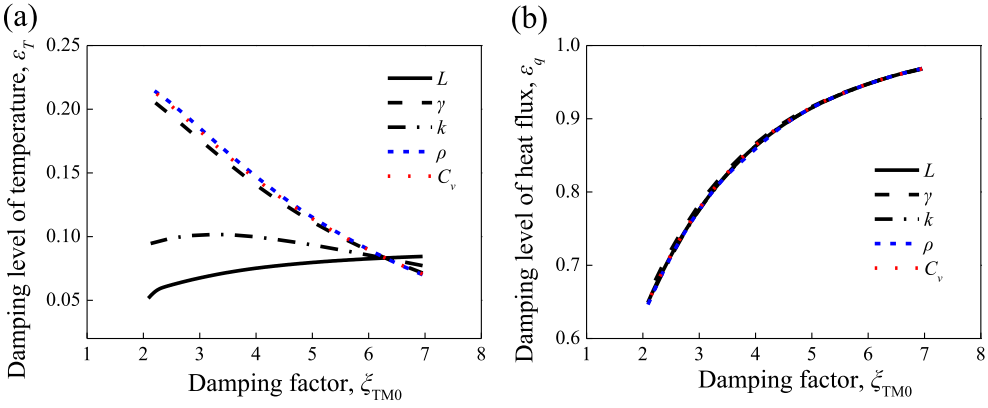

Fig. 6. Effects of the damping factor ξ_{TM0} on the damping levels of the (a) temperature and (b) heat flux predicted by the simplified TM model in Eq. (30), in which the damping factors are varied due to the changes of L, γ, k, ρ and C_v, respectively.

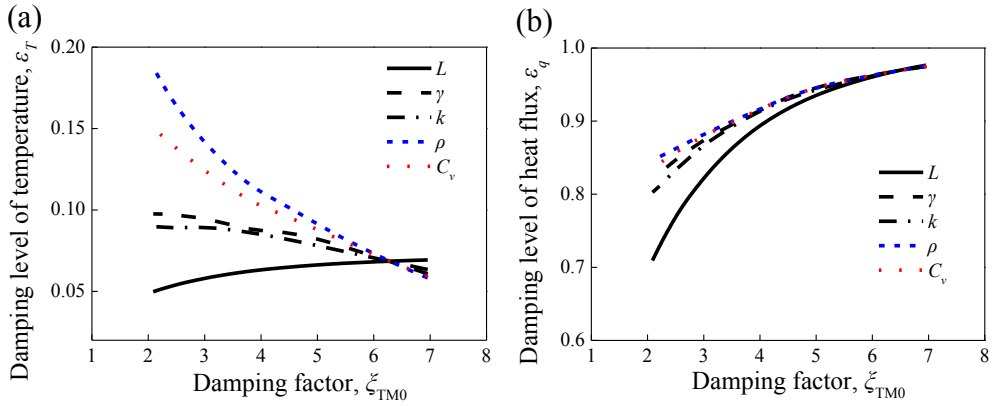

Fig. 7. Effects of the damping factor ξ_{TM0} on the damping levels of the (a) temperature and (b) heat flux predicted by the TM model in Eq. (31), in which the damping factors are varied due to the changes of L, γ, k, ρ and C_v, respectively.

this process, which is similar to those of the inertia term of the temperature gradient to time on the DPL model. Also similar to the DPL model, effects of the damping factor ξ_{TM0} due to the changes of L, γ, k, ρ and C_v separately on the damping level of the heat flux overlap together only when the heat diffusion is strong. The variation trends of the damping level of the temperature with the increase of the damping factor ξ_{TM0} due to the changes of L, γ, k, ρ or C_v is same with those predicted by the simplified TM model.

4.4. Exponential damping

From the Boltzmann relationship [18], we can know that the damping of the energy transported by the thermal wave usually takes the exponential form. The damping of the thermal waves predicted by the CV, DPL and TM models is similar to that of the damped oscillations. For the typical damped oscillations [45], the damping of their amplitudes also takes in the exponential form. For the above considerations, we retreated data about effects of the damping factors ξ_{CV} and ξ_{TM0} on the damping levels of the heat flux predicted by the CV and simplified TM models, respectively. Relationships between the damping factors ξ_{CV}, ξ_{TM0} and $-\ln(1-\varepsilon_q)$ predicted by the CV and simplified TM models are shown in Fig. 8. The common good linearity between the damping factors ξ_{CV}, ξ_{TM0} and $-\ln(1-\varepsilon_q)$ predicted by the CV and simplified TM models confirmed the exponential damping of the thermal waves. Besides, from Fig. 8, we can find that the two slopes predicted by the CV and simplified TM models are both very close to 0.5.

Why the exponential damping happens in this process and the two slopes are very close to 0.5? Taking the CV model again, we will present the reasons. First, we combine the CV model in Eq. (4) and energy conservation equation in Eq. (8) and get the following equation:

$$\tau_q \frac{\partial^2 q}{\partial t^2} + \frac{\partial q}{\partial t} - \alpha \frac{\partial^2 q}{\partial x^2} = 0. \tag{32}$$

Then, using the Fourier analysis method [46], we can define q as

$$q = \sum_{n=-\infty}^{+\infty} A_n(t) e^{\mathrm{i}nx}, \tag{33}$$

where $A_n(t)$ is the amplitude of the wavelet, whose wave number is n, at the time t. i is the imaginary number. $n = 1/\lambda$, in which λ is the wavelength of the corresponding wavelet. Further, substituting the Eq. (33) into the Eq. (32), we can get the relationship:

$$\sum_{n=-\infty}^{+\infty} \left[\tau_q \frac{\partial^2 A_n(t)}{\partial t^2} + \frac{\partial A_n(t)}{\partial t} + \alpha n^2 A_n(t) \right] e^{\mathrm{i}nx} = 0. \tag{34}$$

Considering that the base $\{e^{\mathrm{i}nx}\}$ has linear independence, for the wavelet whose wave number is n, we can always obtain the equation:

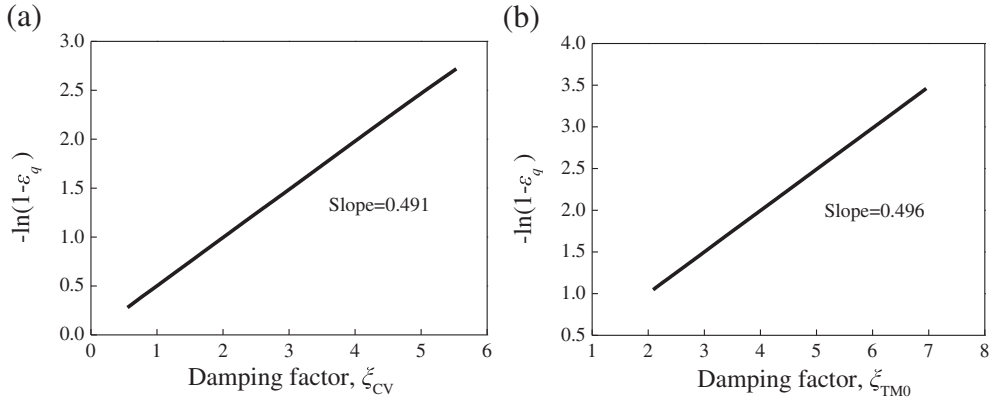

Fig. 8. Relationships between the damping factors (a) ξ_{CV}, (b) ξ_{TM0} and $-\ln(1-\varepsilon_q)$ predicted by the (a) CV and (b) simplified TM models.

Table 2
Conditions for the CV and simplified TM models, in which only the travelling distance L varied.

	k	ρ	C_v	T_0	d	τ_q	τ_T	γ	x^*_{f0}	L
CV-1S	0.1	1.0	1.0	1.0	1.0	0.20	–	–	0.2	Varied
CV-2M	0.4	1.0	1.0	1.0	1.0	0.05	–	–	0.2	Varied
CV-3B	1.0	1.0	1.0	1.0	1.0	0.02	–	–	0.2	Varied
TM-1S	1.0	20.0	1.0	1.0	1.0	–	–	0.1	0.2	Varied
TM-2M	5.0	20.0	1.0	1.0	1.0	–	–	2.5	0.2	Varied
TM-3B	10.0	20.0	1.0	1.0	1.0	–	–	10.0	0.2	Varied

$$\tau_q \frac{\partial^2 A_n(t)}{\partial t^2} + \frac{\partial A_n(t)}{\partial t} + \alpha n^2 A_n(t) = 0, \tag{35}$$

which applies to arbitrary wave number. So, we can find the Eq. (35) is similar to the viscously damped free vibration equation [45]. Using the damped free vibration theory [45], we can get the expressions of $A_n(t)$, as followings:

$$A_n(t) = e^{-\zeta\omega t}\left(C_1 \sin\sqrt{1-\zeta^2}wt + C_2 \cos\sqrt{1-\zeta^2}wt\right), \quad \text{if } \zeta < 1; \tag{36}$$

$$A_n(t) = e^{-\zeta\omega t}(C_3 + C_4 t), \quad \text{if } \zeta = 1; \tag{37}$$

$$A_n(t) = C_5 e^{-\left(\zeta-\sqrt{\zeta^2-1}\right)wt} + C_6 e^{-\left(\zeta+\sqrt{\zeta^2-1}\right)wt}, \quad \text{if } \zeta > 1. \tag{38}$$

Here, ζ is the damping ratio $\frac{1}{2\sqrt{\alpha n^2 \tau_q}}$, and w is the natural angular velocity $\sqrt{\frac{\alpha n^2}{\tau_q}}$. The situations $\zeta < 1$, $\zeta = 1$, and $\zeta > 1$ correspond to the underdamped, critically damped, and overdamped cases. Besides, C_1, C_2, C_3, C_4, C_5, and C_6 are the arbitrary constants determined from the initial conditions. The above analyses are consistent with the thermal vibration phenomena discussed by Xu and Wang [47] for the dual-phase-lagging (DPL) heat conduction model and Cheng et al. [48] for the single-phase-lagging heat conduction model. Xu and Wang [47] also divided the thermal vibration phenomenon into the underdamped, critically damped, and overdamped cases, but their study only focused on the temperature distribution.

For the underdamped case, its amplitude always satisfies the exponential damping relationship. For the critically damped case, its amplitude satisfies the exponential damping relationship only when $C_4 = 0$. For the overdamped case, its amplitude satisfies the exponential damping relationship in most of the propagation process of the thermal wave with the deviation occurring only at the primary stage. Considering the critically damped case is individual and the range of the wave number is from negative infinity to positive infinity, the exponential damping relationship applies to the propagation process of the thermal wave predicted by the CV model in most conditions, with the deviation occurring only when the overdamped cases take a major role and the thermal wave stays at the primary stage of its propagation process.

The situation $\zeta < 1$ takes the form $\alpha n^2 \tau_q > 1/4$, namely $(\alpha\tau_q/\lambda^2) > 1/4$. By observing the thermal waves predicted by the CV and simplified TM models under the base conditions CV-1 and TM-1, we can find that the thermal waves are both very sharp, which means λ is very small and most wavelets stay at the underdamped cases. So, from Eq. (36), we can obtain that

$$\frac{A_n\left(t_{f0} + \frac{L}{\sqrt{\alpha/\tau_q}}\right)\Big|_{\max}}{A_n\left(t_{f0}\right)\Big|_{\max}} = e^{-\frac{1}{2}\frac{L}{\sqrt{\alpha\tau_q}}} = e^{-\frac{1}{2}\xi_{CV}}, \tag{39}$$

where t_{f0} corresponds to the time when the wave frontier reaches x_{f0}. Since the coefficient for the amplitude of each wavelet with the damping factor ξ_{CV} is 0.5 and the critically damped and overdamped cases can affect the coefficient, the slope of $-\ln(1-\varepsilon_q)$ predicted by the CV model to the damping factor ξ_{CV} is near 0.5, as shown in Fig. 8(a). Considering the similarity between the CV and simplified TM models, the above analyses and conclusions also apply to the simplified TM model.

4.5. Sharp and blunt thermal waves

From the above discussion, we can find that when the thermal waves predicted by the CV and simplified TM models are blunt, the overdamped cases will increase and the corresponding slope of $-\ln(1-\varepsilon_q)$ to the damping factor ξ_{CV} will change. So, we need to compare the propagation behaviours of the sharp and blunt thermal waves. Here, the sharp thermal wave means that the amplitude of the thermal wave is high while its bottom width is small, and the blunt thermal wave corresponds to the contrary. For the above considerations, we design conditions in Table 2 for the CV and simplified TM models, in which only the travelling distance L varied. Conditions CV-1S, CV-2M, and CV-3B correspond to a group of sharp, medium, and blunt thermal waves predicted by the CV model. Conditions TM-1S, TM-2M, and TM-3B correspond to a

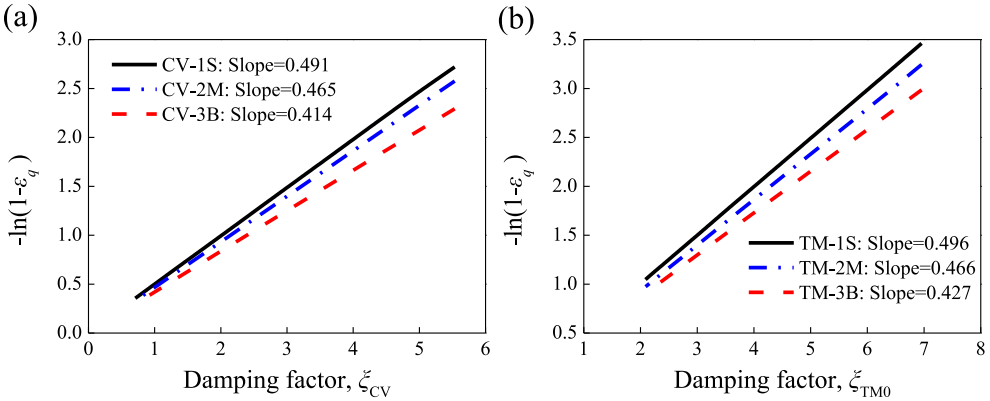

Fig. 9. Relationships between the damping factors (a) ξ_{CV}, (b) ξ_{TM0} and $-\ln(1-\varepsilon_q)$ predicted by the (a) CV and (b) simplified TM models under three situations: sharp, medium, and blunt thermal waves.

group of sharp, medium, and blunt thermal waves predicted by the simplified TM model.

Fig. 9 presents the relationships between the damping factors ξ_{CV}, ξ_{TM0} and $-\ln(1-\varepsilon_q)$ predicted by the CV and simplified TM models under three situations: sharp, medium, and blunt thermal waves. It can be seen that for the CV and simplified TM models, the sharp, medium, and blunt thermal waves predict different slopes of $-\ln(1-\varepsilon_q)$ to the corresponding damping factor and different $-\ln(1-\varepsilon_q)$ under the same damping factor, namely different damping levels of heat flux under the same damping factor. This is due to the increase of overdamped cases when the bottom width of the thermal wave increases, which changes the slope of $-\ln(1-\varepsilon_q)$ to the corresponding damping factor and makes that the damping factors ξ_{CV} and ξ_{TM} cannot be the characteristic numbers for determining the damping of the thermal waves predicted by the CV and simplified TM models.

5. Conclusions

The damping levels of temperature and heat flux (ε_T, ε_q) were defined for evaluating the damping of the thermal waves predicted by the CV, DPL, and TM models. The damping level of the heat flux is found to be a better factor for this because the heat flux is directly related to the energy transported by the thermal wave while the temperature can be also affected by the thermal properties. The damping factor ξ ($L/\sqrt{\alpha\tau}$) was defined for determining the damping of the thermal waves predicted by the CV, DPL, and TM models, where L is the travelling distance of the thermal wave, α is the thermal diffusivity, and τ is the corresponding relaxation time. ξ represents the ratio of the time that the thermal wave needs to travel the distance L to the relaxation time, or $\sqrt{3}$ times of the reciprocal of the Knudsen number.

For the sharp thermal waves predicted by the CV and simplified TM models, the damping factors ξ_{CV} and ξ_{TM} can be the characteristic numbers that has a decisive impact on the damping level of the heat flux, in which the simplified TM model only retain the inertia term of the heat flux to time while neglecting the inertia term of the temperature to time and nonlocal terms in the TM model. But if both including the sharp and blunt thermal waves, the increase of overdamped cases under the blunt thermal wave situation will lead to the deviation for the characteristic numbers. For the sharp thermal waves predicted by the DPL and TM models, the damping factors ξ_{DPL} and ξ_{TM} cannot be the characteristic numbers, which is due to the impacts on the propagation speed of the thermal wave and its heat diffusion caused by the inertia term of the temperature gradient to time for the DPL model, and the inertia term of the temperature to time and nonlocal terms for the TM model, respectively.

For the thermal waves predicted by the CV and simplified TM models, their propagation processes satisfy the exponential damping relationship in most situations, with the deviation occurring only when the overdamped cases play a major role and the thermal waves stay at the primary stage. Besides, the sharp and blunt thermal waves predict different slopes of $-\ln(1-\varepsilon_q)$ to the damping factor ξ. If the thermal wave is sharper, the overdamped cases are fewer, and therefore the corresponding slope of $-\ln(1-\varepsilon_q)$ to ξ is closer to 0.5.

Acknowledgements

This work was financially supported by National Natural Science Foundation of China (Nos. 51322603, 51136001, 51176099, 51356001, 51321002), Program for New Century Excellent Talents in University, Tsinghua University Initiative Scientific Research Program.

References

[1] J. Fourier, The Analytical Theory of Heat, Dove Publications, Inc., New York, 1955.
[2] R. Shirmohammadi, Temperature transients in spherical medium irradiated by laser pulse, Int. Commun. Heat Mass Transf. 35 (2008) 1017–1023.
[3] T.T. Lam, Thermal propagation in solids due to surface laser pulsation and oscillation, Int. J. Therm. Sci. 49 (2010) 1639–1648.
[4] M.T. Xu, J.F. Guo, L.Q. Wang, L. Cheng, Thermal wave interference as the origin of the overshooting phenomenon in dual-phase-lagging heat conduction, Int. J. Therm. Sci. 50 (2011) 825–830.
[5] D.Y. Tzou, Experimental support for the lagging behavior in heat propagation, AIAA J. Thermophys. Heat Transf. 9 (1995) 686–693.
[6] P. Zhang, M. Murakami, R.Z. Wang, Study of the transient thermal wave heat transfer in a channel immersed in a bath of superfluid helium, Int. J. Heat Mass Transf. 49 (2006) 1384–1394.
[7] K.J. Hays-Stang, A. Haji-Sheikh, A unified solution for heat conduction in thin films, Int. J. Heat Mass Transf. 42 (1999) 455–465.
[8] C.W. Chang, D. Okawa, H. Garcia, A. Majumdar, A. Zettl, Breakdown of Fourier's law in nanotube thermal conductors, Phys. Rev. Lett. 101 (2008) 075903.
[9] J. Ordonez-Miranda, J.J. Alvarado-Gil, Thermal wave oscillations and thermal relaxation time determination in a hyperbolic heat transport model, Int. J. Therm. Sci. 48 (2009) 2053–2062.
[10] K.C. Liu, Thermal propagation analysis for living tissue with surface heating, Int. J. Therm. Sci. 44 (2008) 507–513.
[11] J. Fan, L.Q. Wang, Analytical theory of bioheat transport, J. Appl. Phys. 109 (2011) 104702.
[12] Y. Dong, B.Y. Cao, Z.Y. Guo, General expression for entropy production in transport processes based on the thermomass model, Phys. Rev. E 85 (2012) 061107.
[13] V.A. Cimmelli, A. Sellitto, D. Jou, Nonlocal effects and second in a nonequilibrium steady state, Phys. Rev. B 79 (2009) 014303.
[14] D.Y. Tzou, Z.Y. Guo, Nonlocal behavior in thermal lagging, Int. J. Therm. Sci. 49 (2010) 1133–1137.
[15] D.D. Joseph, L. Preziosi, Heat waves, Rev. Mod. Phys. 61 (1989) 41–74.
[16] A.E. Kronberg, A.H. Benneker, K.R. Westerterp, Notes on wave theory in heat conduction: a new boundary conduction, Int. J. Heat Mass Transf. 41 (1998) 127–137.
[17] D. Jou, V.A. Cimmelli, A. Sellitto, Nonequilibrium and second-sound propagation along nanowires and thin layers, Phys. Lett. A 373 (2009) 4386–4392.
[18] G. Chen, Ballistic-diffusive heat-conduction equations, Phys. Rev. Lett. 86 (2001) 2297.
[19] B. Straughan, Heat Waves, Springer, New York, 2011.
[20] G. Lebon, H. Machrafi, M. Grmela, Ch. Dubois, An extended thermodynamic model of transient heat conduction at sub-continuum scales, Proc. R. Soc. A 467 (2011) 3241–3256.
[21] C. Cattaneo, Sur uneforme de l'Equation de la chaleurelinant le paradoxed'une propagation instantance, C.R. Acad. Sci. Paris 247 (1958) 431–433.
[22] M.P. Vernotte, Les paradoxes de la theorie continue de l'equation de la chaleur, C.R. Acad. Sci. Paris 246 (1958) 3154–3155.
[23] D.Y. Tzou, The generalized lagging response in small-scales and high-rate heating, Int. J. Heat Mass Transf. 38 (1995) 3231–3240.
[24] D.Y. Tzou, A unified field approach for heat conduction from micro- to macroscales, ASME J. Heat Transf. 117 (1995) 8–16.
[25] J.K. Chen, J.E. Beraun, D.Y. Tzou, A dual-phase-lag diffusion model for predicting intermetallic compound layer growth in solder joints, ASME J. Heat Transf. 123 (2001) 52–57.
[26] R.A. Guyer, J.A. Krumhansl, Solution of the linearized phonon Boltzmann equation, Phys. Rev. 148 (1966) 766–778.
[27] R.A. Guyer, J.A. Krumhansl, Thermal conductivity, second sound, and phonon hydrodynamic phenomena in nonmetallic crystals, Phys. Rev. 148 (1966) 778–788.
[28] Z.Y. Guo, Q.W. Hou, Thermal wave based on the thermomass model, ASME J. Heat Transf. 132 (2010) 072403.
[29] Y. Dong, B.Y. Cao, Z.Y. Guo, Generalized heat conduction laws based on thermomass theory and phonon hydrodynamics, J. Appl. Phys. 110 (2011) 063504.
[30] T.T. Lam, E. Fong, Heat diffusion vs. wave propagation in solids subjected to exponentially-decaying heat source: analytical solution, Int. J. Therm. Sci. 50 (2011) 2104–2116.
[31] L.Q. Wang, X.H. Wei, Equivalence between dual-phase-lagging and two-phase-system heat conduction processes, Int. J. Heat Mass Transf. 51 (2008) 1751–1756.
[32] D.Y. Tzou, Nonlocal behavior in phonon transport, Int. J. Heat Mass Transf. 54 (2011) 475–481.
[33] D.W. Tang, N. Araki, Non-Fourier heat conduction behavior in finite mediums under pulse surface heating, Mater. Sci. Eng. A 292 (2000) 173–178.
[34] R.F. Hu, B.Y. Cao, Study on thermal wave based on the thermal mass theory, Sci. China, Ser. E 52 (2009) 1786–1792.
[35] M.R. Wang, N. Yang, Z.Y. Guo, Non-Fourier heat conductions in nanomaterials, J. Appl. Phys. 110 (2011) 064310.
[36] D.W. Tang, N. Araki, Wavy, wavelike, diffusive thermal responses of finite rigid slabs to high-speed heating of laser-pulses, Int. J. Heat Mass Transf. 42 (1999) 855–860.
[37] K. Ramadan, Semi-analytical solution for the dual phase lag heat conduction in multilayered media, Int. J. Therm. Sci. 48 (2009) 14–25.

[38] D. Jou, J.C. Vazquez, G. Lebon, Extended irreversible thermodynamics of heat transport a brief introduction, P. Est. Acad. Sci. 57 (2008) 118–126.
[39] T.T. Lam, A unified solution of several heat conduction models, Int. J. Heat Mass Transf. 56 (2013) 653–666.
[40] W.B. Lor, H.S. Chu, Hyperbolic heat conduction in thin-film high T_c superconductors with interface thermal resistance, Cryogenics 39 (1999) 739–750.
[41] H.Q. Yang, Characteristics-based, high-order accurate and nonoscillatory numerical method for hyperbolic heat conduction, Numer. Heat Transf., Part B 18 (1990) 221–241.
[42] B. Shen, P. Zhang, Notable physical anomalies manifested in non-Fourier heat conduction model under the dual-phase-lag model, Int. J. Heat Mass Transf. 51 (2008) 1713–1727.
[43] J.Z. Zhang, Advanced Heat Transfer, Science Press, Beijing, 2009.
[44] M.K. Zhang, B.Y. Cao, Y.C. Guo, Numerical studies on dispersion of thermal waves, Int. J. Heat Mass Transf. 67 (2013) 1072–1082.
[45] W.T. Thomson, M.D. Dahleh, Theory of Vibration with Applications, Tsinghua University Press, Beijing, 2005.
[46] S.T. Xiao, J.H. Zheng, Calculus (II), Higher Education Press, Beijing, 2003.
[47] M.T. Xu, L.Q. Wang, Thermal oscillation and resonance in dual-phase-lagging heat conduction, Int. J. Heat Mass Transf. 45 (2002) 1055–1061.
[48] L. Cheng, M.T. Xu, L.Q. Wang, Thermal vibration phenomenon of single phase lagging heat conduction and its thermodynamic basis, Chin. Sci. Bull. 53 (2008) 3597–3602.